# Free ethynylarsinidene and ethynylstibinidene: Heavier analogues of nitrenes and phosphinidenes

Arun-Libertsen Lawzer, Elavenil Ganesan, Marcin Gronowski, Thomas Custer, Jean-Claude Guillemin, Robert Kolos

10.1002/chem.202300887

WILEY-VCH

RESEARCH ARTICLE

# Free ethynylarsinidene and ethynylstibinidene: Heavier analogues of nitrenes and phosphinidenes

Arun-Libertsen Lawzer,*[a] Elavenil Ganesan,[a] Marcin Gronowski,[a] Thomas Custer,[a] Jean-Claude Guillemin,[b] and Robert Kołos[a]

[a] Dr. Arun-Libertsen Lawzer
Institute of Physical Chemistry, Polish Academy of Sciences
Kasprzaka 44/52
01-224 Warsaw, Poland
E-mail: alawzer@ichf.edu.pl
[a] Elavenil Ganesan
Institute of Physical Chemistry, Polish Academy of Sciences
Kasprzaka 44/52
01-224 Warsaw, Poland
E-mail: eganesan@ichf.edu.pl
[a] Dr. Marcin Gronowski
Institute of Physical Chemistry, Polish Academy of Sciences
Kasprzaka 44/52
01-224 Warsaw, Poland
E-mail: mgronowski@ichf.edu.pl
[a] Dr. Thomas Custer
Institute of Physical Chemistry, Polish Academy of Sciences
Kasprzaka 44/52
01-224 Warsaw, Poland
Email: thomas.custer@ichf.edu.pl
[a] Prof. Dr. Robert Kołos
Institute of Physical Chemistry, Polish Academy of Sciences
Kasprzaka 44/52
01-224 Warsaw, Poland
Email: rkolos@ichf.edu.pl
[b] Prof. Dr. Jean-Claude Guillemin
Univ Rennes
Ecole Nationale Supérieure de Chimie de Rennes
CNRS, IRCR-UMR 6226
F-35000 Rennes, France
Email : jean-claude.guillemin@ensc-rennes.fr

Supporting information for this article is given via a link at the end of the document.

**Abstract:** Until now, there has been very little experimental evidence for the existence of free arsinidenes and stibinidenes, apart from the hydrides, AsH and SbH. Here we report on photogeneration of triplet ethynylarsinidene, HCCAs, and triplet ethynylstibinidene, HCCSb, from ethynylarsine and ethynylstibine, respectively, in solid argon matrices. The products were identified using infrared spectroscopy and the associated UV absorption spectra are interpreted with the aid of theoretical predictions.

## Introduction

Pnictinidenes are molecules containing a monovalent group 15 (pnictogen) atom. Unless efficiently stabilized by an electron-rich π-donating substituent,[1] most of them have triplet ground electronic states. Nitrenes, the archetypal representatives of pnictinidenes, are widely studied in organic reactions.[2] Moving down group 15, several triplet phosphinidenes[3] have been generated and characterized in argon matrices. The hydrides NH[4], PH,[5] AsH,[6] SbH,[7] and BiH[8] have all been generated via degradation of their respective $NH_3$, $PH_3$, $AsH_3$, $SbH_3$ and $BiH_3$ precursors. Below phosphorus in group 15, however, methylbismuthinidene, $CH_3Bi$,[9] and methylarsinidene, $CH_3As$[10] are the only polyatomic pnictinidenes so far characterized experimentally and are generated by gas-phase pyrolysis of their corresponding trimethyl precursor. Synthesis of free stable pnictinidenes is an active area of research. The electron deficiency at a pnictogen atom makes them highly reactive, and the only way to synthesize a stable compound is with a π-donating, bulky, electron-rich substituent which shields and stabilises the pnictinidene site.

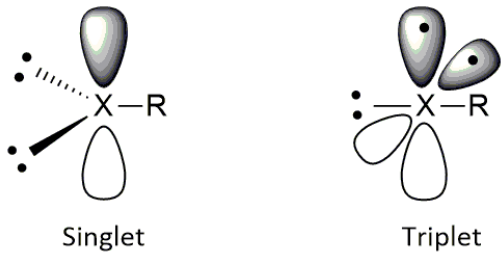


**Scheme 1**. Electronic structure of pnictinidenes. Half-filled and empty p-orbitals of the pnictogen (X) atom are shown. Bars marked with two dots symbolise hybridized orbitals of the lone pairs.

Apart from a few nitrenes stable at room temperature,[11] only one such pnictinidene (a phosphino-phosphinidene) has been synthesized.[12] Attempts to synthesize arsinidenes or

10.1002/chem.202300887




stibinidenes have typically resulted in dimerization, even with bulky substituents shielding the pnictogen moiety.[13] Monomeric forms have been produced only as singlet Lewis adducts, using inter- or intramolecular electron donors.[14] We have demonstrated[15] that ethynylphosphine, generated from phosphapropyne in a rare gas matrix, undergoes UV-induced dehydrogenation to form triplet ethynylphosphinidene, HCCP. It was of interest to find out whether a similar photochemical process could produce the analogous compounds HCCAs and HCCSb. Here we report on the generation of free ethynylarsinidene and ethynylstibinidene in cryogenic argon matrices. These molecules are characterized using IR and UV/Visible spectroscopy together with theoretical predictions.

## Results and Discussion

Unlike ethynylphosphine, both pnictines used here as photochemical precursors, $HCCAsH_2$ and $HCCSbH_2$, are highly unstable. Experiments were carried out promptly following their synthesis, after brief storage at 77 K. Details pertaining to the preparative synthesis, cryogenic technique, UV irradiation, and spectroscopic measurements are provided in the experimental section. Briefly, the pnictines, $HCCAsH_2$ and $HCCSbH_2$, were obtained from the respective ethynyldichloro-derivatives using tributyltin as a reducing agent.[16] The pnictine vapor was mixed with argon at a ratio of 1:1000. The mixture, trapped at 6 K as a solid layer on an optical window inside a cryostat, was subjected to UV photolysis and analyzed with IR and UV/Visible absorption spectroscopy.

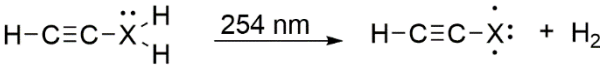


**Scheme 2**. Photogeneration of triplet ethynylpnictinidenes. X stands for P, As, or Sb atoms.

Representative IR spectra following the photolyses of $HCCAsH_2$ and $HCCSbH_2$ are shown in Fig. 1. Our assignments of the ethynylpnictinidene bands in Fig. 1 and Tab. 1 are based on the DFT-predicted anharmonic vibrational frequencies and IR intensities. The time evolution of these IR bands (SI, Fig. S1) further supports their assignment. After 60 h of Hg-lamp irradiation, the concentration of arsinidene was still increasing, albeit weakly, while that of stibinidene passed through a broad maximum after just 2 h (Fig. 2). Such dissimilar photochemical susceptibilities may stem from different cross-sections for the applied 254 nm radiation or from different yields of the ensuing dehydrogenation reactions. For both pnictines, however, the UV absorption at that wavelength was too weak to allow a standard spectrophotometric measurement of optical density (the same was true for ethynylphosphine[15]).

We have also detected the IR spectral features attributable[17] to the highest frequency stretching modes of CCAs (1692 $cm^{-1}$) and CCSb (1751 $cm^{-1}$). Unlike the bands of pnictinidenes, they grow approximately linearly (SI, Figure S1), starting from the onset of the photolysis. This suggests a precursor for CCX whose concentration is nearly constant over the course of the observed experimental period. This steady-state species could be excited state [HCCX]* which is formed from either dehydrogenation of excited $[HCCXH_2]$* or from photoexcitation of HCCX. Theory predicts these $\nu_1$ bands to be the most intense for both radicals (SI, Table. S3). Based on theoretically derived absolute intensities of the observed IR bands (Table 1 and S3), the concentrations of CCX radicals in extensively photolyzed samples were found to be approximately 30 and 65 times lower than that of HCCX molecules, for As- and Sb-bearing species, respectively.

Our previous study showed that ethynylphosphine photo-rearranges to phosphapropyne and phosphaallene and that this rearrangement occurs concurrently with dehydrogenation.[15] However, we observed no photoisomerization of the arsine or the stibine precursors ($HCCAsH_2$ and $HCCSbH_2$). We could not detect any isomers of HCCAs or HCCSb (or of HCCP [15]), while the photochemical generation of the nitrene, HCCN, in solid argon was reportedly[18] accompanied by formation of HCNC and cyclo-CHCN.

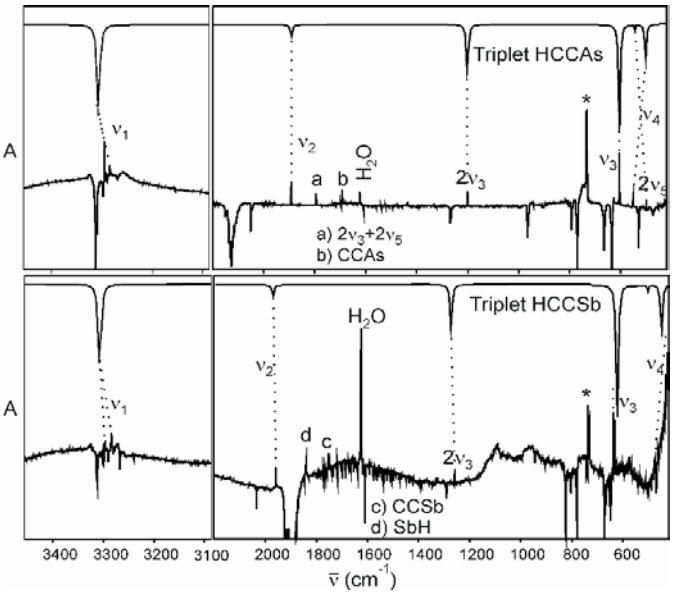


**Figure 1.** Top : IR absorption spectrum theoretically derived (anharmonic approach : VPT2//B3LYP with basis sets aug-cc-pVTZ for H and C; aug-cc-pVTZ-PP for As And Sb) for the ground electronic state of HCCAs, compared with a difference spectrum (after-minus-before photolysis) showing the result of a prolonged (3 days) Hg-lamp irradiation of $HCCAsH_2$ isolated in solid Ar. Bottom: analogous spectra depicting the identification of HCCSb as the product of $HCCSbH_2$/Ar photolysis; irradiation time: 4 h. Bands of the theoretically predicted spectra pointing downwards to facilitate the comparison with experimental results. Asterisk indicates an artefact feature originating in the CsI substrate window.

The electronic structure of HCCN is not that of a nitrene (H—C≡C—N̤·) but of cyanocarbene[18] (H—·C·—C≡N̤) with a significant allenic (H—Ċ=C=N̤) admixture. Moving from P to Sb, the allenic contribution decreases, the carbenic one is non-significant, and the pnictinidene character (H—C≡C—Ẍ·) prevails. This trend, the increase in acetylenic character of the C-C bond on moving towards a heavier species, is demonstrated by an increase in the C-C stretching frequency: 1734 $cm^{-1}$ for HCCN[18] to 1787 $cm^{-1}$ for HCCP[15] to 1893 $cm^{-1}$ for HCCAs to 1955 $cm^{-1}$ for HCCSb. While large changes in the C-H bond are not expected, the increase in acetylenic nature of the CCH unit can still be seen in the growing CH stretching frequencies: 3229 $cm^{-1}$ for HCCN[18], 3288 $cm^{-1}$ for HCCP[15], 3294 $cm^{-1}$ for HCCAs, 3297 $cm^{-1}$ for HCCSb. The HCC bending frequency exhibits a system-

**Table 1.** IR-spectroscopic identification of the triplet pnictinidenes HCCAs and HCCSb.

| Vibrational Mode | | HCCAs | | | | HCCSb | | | |
|---|---|---|---|---|---|---|---|---|---|
| | | Theory (anharmonic)[a] | | Experimental (argon matrix) | | Theory (anharmonic)[a] | | Experimental (argon matrix) | |
| | | Frequency ($cm^{-1}$) | Intensity (km $mol^{-1}$) | Frequency ($cm^{-1}$) | Relative Intensity (%) | Frequency ($cm^{-1}$) | Intensity (km $mol^{-1}$) | Frequency ($cm^{-1}$) | Relative Intensity (%) |
| ν1 | CH stretching | 3310 | 61 | 3294.7<br>3284.6 | 100 | 3314 | 54 | 3297.0<br>3283.9 | 60 |
| ν2 | CC stretching | 1890 | 8.8 | 1893.1 | 13 | 1975 | 9.7 | 1955.9 | 18 |
| 2ν3 | overtone | 1214 | 37 | 1201.0 | 17 | 1298 | 35 | 1256.7 | 26 |
| ν3 | CCH bending | 609 | 72 | 605.9 | 59 | 652 | 74 | 635.1 | 100 |
| ν4 | CX stretching | 508 | 22 | 552.9 | 10 | 431 | 34 | 473.3 | 21 |
| 2ν5 | overtone | 549 | 0.1 | 498.7 | 6 | 471 | 0.3 | Not observed | |
| ν5 | CCX bending | 271 | 25 | Out of detection range | | 232 | 27 | Out of detection range | |

[a] VPT2//B3LYP with basis sets aug-cc-pVTZ for H, C, P and aug-cc-pVTZ-PP for As, Sb.

-atic increase in energy moving from HCCN to HCCSb: 458 $cm^{-1}$ [18c] (or lower)[18a] for HCCN, 565 $cm^{-1}$ for HCCP[15], 606 $cm^{-1}$ for HCCAs, and 635 $cm^{-1}$ for HCCSb. This indicates that the unpaired electron density becomes more localized on the pnictogen atom of HCCX when moving from nitrogen- to antimony-bearing molecules. These increasing frequencies show that the electronic structure plays a dominant role compared to the contribution from the mass of the pnictogen atom. For C-X stretching (1735 $cm^{-1}$ for HCCN[18], 696.1 $cm^{-1}$ for HCCP[15], 552.9 $cm^{-1}$ for HCCAs, and 473.3 $cm^{-1}$ for HCCSb), the electronic structure and the mass of the pnictogen both cause a trend towards lower frequencies.

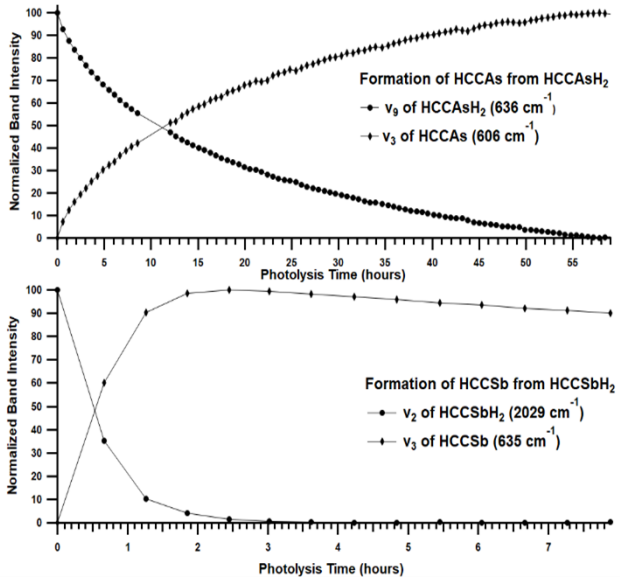


**Figure 2.** Comparison of time evolution of IR band intensities over the course of 254 nm photolysis of $HCCAsH_2$ (top panel) and $HCCSbH_2$ (bottom panel). Intensities of precursor and product bands are normalized (100 being assigned to the maximal value observed for each band). The degradation of $HCCAsH_2$ was not complete after the total photolysis time of 60 h. To correct for that, the residual intensity measured at the end of irradiation was subtracted prior to the normalization. Bands $\nu_9$ and $\nu_3$ are the C-H bending modes of the corresponding molecules. In the case of $HCCSbH_2$, the bending C-H and Sb-H frequencies are overlapping, therefore the $\nu_2$ (C-C stretching) band was traced.

The theoretical predictions show an increase of the CC bond order (Table 2), while moving towards the heavier pnictinidene which is consistent with the changes of the CC stretching frequencies discussed earlier. The lack of efficient orbital overlap between the acetylenic unit and the pnictinidene center in heavier pnictinidenes is illustrated in Fig. 3 by in the contour maps of the highest occupied (HOMO) and singly occupied (SOMO) molecular orbitals.

The electronic structure of HCCX (X=P, As, Sb) molecules is determined by two electrons distributed on the two degenerate $\pi^*$ molecular orbitals. Therefore, HCCX species have a triplet ground state, as we expect based on Hund's rule. DFT predicted triplet-singlet energy gaps of HCCP, HCCAs, HCCSb, and HCCBi are all similar: 22, 23, 22, and 21 kcal $mol^{-1}$, respectively.

**Table 2.** Bond length (Å), bond order and electric dipole moment (Debye) of HCCX molecules obtained with B3LYP and CCSD. The bond orders are reported only for B3LYP. Augmented triple-zeta basis sets were applied.

| Species | Bond length (Bond order) | | | Dipole moment |
|---|---|---|---|---|
| | H-C | C-C | C-X | |
| HCCN | 0.998* | 1.323* | 1.195* | *3.25* |
| HCCP | 1.057*<br>*1.063* (*0.99*)<br>{1.065} | 1.241*<br>*1.229* (*2.78*)<br>{1.231} | 1.685*<br>*1.685* (*0.99*)<br>{1.702} | *1.18*<br>{1.24} |
| HCCAs | *1.063* (*0.99*)<br>{1.065} | *1.220* (*2.83*)<br>{1.225} | *1.840* (*0.99*)<br>{1.840} | *0.52*<br>{0.53} |
| HCCSb | *1.063* (*0.99*)<br>{1.065} | *1.215* (*2.89*)<br>{1.221} | *2.062* (*0.99*)<br>{2.056} | *0.16*<br>{0.16} |

* Values measured with microwave spectroscopy.[19] Values in italics and within { } were obtained with B3LYP and CCSD calculations, respectively.

The excited electronic states were explored using *ab initio* relativistic electronic structure methods. All energies and properties were computed using the vertical approximation based on the ground-state geometry predicted at CCSD level of theory. The excitation energies were obtained with Fock-space CCSD (FS-CCSD)[20] and the generalized active space configuration interaction (GASCI) method.[21] Both approaches predict that the first and second singlet states of HCCX molecules lie at 18-21 kcal/mol and 33-39 kcal/mol above the ground state, respectively (Table 3). With increasing mass, relativistic effects, including spin-orbit interaction, become increasingly important. The energy

10.1002/chem.202300887




**Table 3.** Excitation energies and transition dipole moments from the ground state obtained by Generalized Active Space Configuration Interaction (GASCI) and Fock-space CCSD (FS-CCSD, inside the parentheses) calculations.

| State | | | HCCP | | HCCAs | | HCCSb | |
|---|---|---|---|---|---|---|---|---|
| | | | Relative energy $cm^{-1}$ | Transition dipole moment Debye | Relative energy $cm^{-1}$ | Transition dipole moment Debye | Relative energy $cm^{-1}$ | Transition dipole moment Debye |
| Triplets | $X^3\Sigma^-$ | Ω=0 | 0(0) | - | 0 (0) | - | 0 (0) | - |
| | | Ω=1 | 4.2(4.6) | 0.0001 | 110 (124) | 0.003 | 636 (660) | 0.02 |
| | $1^3\Delta$ | Ω=3 | 30522 (30717) | - | 30191 (30742) | - | 30283 (32273) | - |
| | | Ω=2 | 30636 (30828) | - | 30692 (31236) | - | 31316 (33284) | - |
| | | Ω=1 | 30751 (30940) | 0.002 | 31227 (31759) | 0.01 | 31568 (33379) | 0.04 |
| | $1^3\Sigma^+$ | Ω=1 | 31850 (32039) | 0.001 | 31696 (32244) | 0.008 | 32715 (34617) | 0.02 |
| | | Ω=0 | 31857 (32044) | - | 31924 (32413) | - | 32851 (34459) | - |
| | $1^3\Sigma^-$ | Ω=0 | 33580 (34578) | 1.9 | 32984 (34155) | 2.0 | 32920 (34831) | 2.0 |
| | | Ω=1 | 33584 (33580) | 0.003 | 33157 (34269) | 0.01 | 33918 (35665) | 0.03 |
| | $1^3\Pi$ | Ω=2 | 40491 (37099) | - | 41678 | - | 38760 | - |
| | | Ω=1 | 40594 (37210) | 0.9 | 42204 | 0.9 | 39851 | 1.1 |
| | | Ω=0 | 40704 (37322) | - | 42813 | - | 41424 | - |
| Singlets | $1^1\Delta$ | | 6499 (6233) | - | 6902 (6429) | - | 7339 (7519) | - |
| | $1^1\Sigma^+$ | | 11542 (11643) | 0.004 | 12439 (12409) | 0.01 | 13471 (14022) | 0.03 |
| | $1^1\Sigma^-$ | | 28588 (28389) | - | 28667 (28932) | - | 29356 (30602) | - |

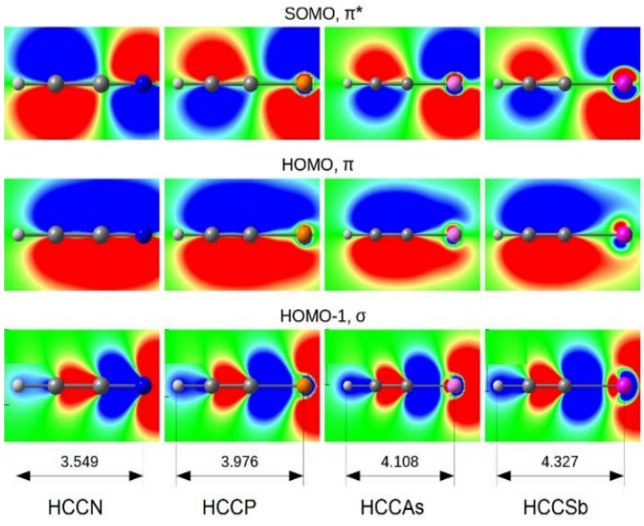


**Figure 3.** DFT-derived (restricted-open-B972, augmented triple-zeta basis set) frontier molecular orbitals. Lengths in Å.

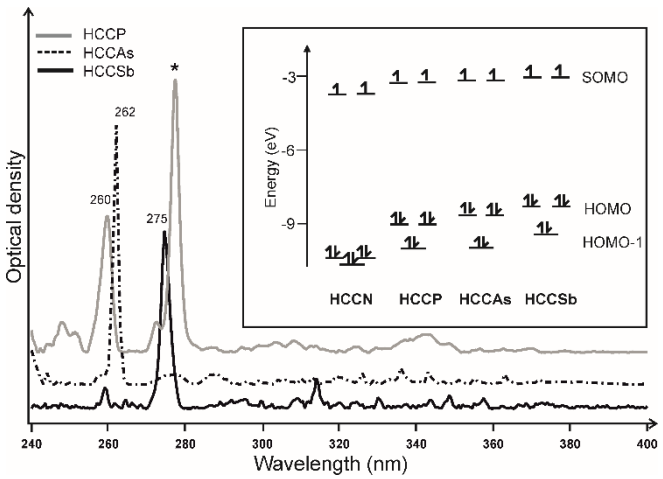


**Figure 4.** UV absorption spectra obtained after 254 nm photolysis of $HCCSbH_2$ (bottom) and $HCCAsH_2$ (middle). Spectrum of HCCP (top) is reproduced from Ref. 14. Asterisk marks an unidentified photoproduct uncorrelated to HCCP. Energies of the frontier molecular orbitals (inset) were obtained by restricted-open-B972 computation with augmented triple zeta basis set.

difference between Ω=1 and Ω=O components of the ground electronic state grows from 4 $cm^{-1}$ (for HCCP) to about 650 $cm^{-1}$ (for HCCSb) (Table 3), yet the spin-orbit splitting does not change the energetic order of the states $X^3\Sigma^-$, $1^1\Delta$ and $1^1\Sigma^+$. CASSCF calculations show similar results (SI, S5).

The electronic spectra of ethynylpnictinidenes exhibit a multiplet structure spread over the range of approx. 290 to 380 nm. We assign these features to the vibronic bands of the first fully allowed electronic transition, $X^3\Sigma^- \rightarrow 1^3\Sigma^-$ (Table 3), shaped mostly by the HOMO-SOMO ($\sigma^2\pi^4\pi^{*2} \rightarrow \sigma^2\pi^3\pi^{*3}$) excitation. The corresponding origin bands are likely in the region of 350 to 370 nm (28 600 to 27 000 $cm^{-1}$); if so, the corresponding theoretically predicted transition energies would be higher by about 0.7-0.8 eV (Table 3). In HCCN, the analogous π-π* system (identified as $X^3\Sigma \rightarrow 1^3\Sigma^{-1}$) [18d], appears around 300 to 340 nm with a vibronic progression of ca. 550 $cm^{-1}$.[18]

The expected second fully allowed transition is $X^3\Sigma^- \rightarrow 1^3\Pi$, associated mostly with the change of electronic configuration from $\sigma^2\pi^4\pi^{*2}$ to $\sigma^1\pi^4\pi^{*3}$. As illustrated by the scheme of orbitals (inset of Fig. 4), energies of such HOMO-1 to SOMO excitations are likely similar for HCCP and HCCAs. This is reflected in the experimentally observed peak wavelengths: 260 nm and 262 nm, respectively. For HCCSb, the transition is slightly red-shifted (to 274 nm), in qualitative agreement with the predicted orbital energies. These strong absorption features can be reasonably assigned to the 0-0 bands of the $X^3\Sigma^- \rightarrow 1^3\Pi$ systems. The corresponding theoretically predicted transition energies (Table 3)

are higher by approximately 2130, 4040, and 3360 $cm^{-1}$ (0.26, 0.5, and 0.42 eV) for HCCP, HCCAs and HCCSb, respectively. In HCCN, where the carbene structure prevails (i.e. the carbon atom of CH-moiety has most of the unpaired electron density[23]), the transition analogous to $X^3\Sigma^- \rightarrow 1^3\Pi$ appears as a vibronic progression between 295 nm and 240 nm (spacing of ca. 1100 $cm^{-1}$ is probably due to CCN stretching).[18] However, HCCP, HCCAs, and HCCSb, with their unpaired electrons localized mostly on the pnictogen atom, show a clear resemblance to NH[4], PH[5], AsH[6], SbH[7], and BiH[8]. For these diatomic pnictinidenes, the observed origin bands of the $X^3\Sigma^- \rightarrow 1^3\Pi$ system ($\sigma$-$\pi^*$) all fall in a narrow wavelength range, around 340 nm.

## Conclusion

In summary, photodehydrogenation of $HCCAsH_2$ and $HCCSbH_2$, carried out in argon matrices, produced the triplet arsinidene HCCAs and stibinidene HCCSb. Both were identified and characterized using infrared spectroscopy. The fact that we did not observe HCCAsH and HCCSbH radicals suggests that HCCAs and HCCSb are formed through a concerted loss of $H_2$ and that the photodehydrogenation reaction might be a viable method for a synthetic chemist to generate these species in solution and stabilize them with a suitable ligand. We have compared the IR and UV absorption spectra of HCCAs and HCCSb with those of HCCN and HCCP to understand the changes in electronic structure. Both theoretical and IR spectroscopic investigations indicate that the monovalent character of a pnictogen atom is more pronounced for the HCCAs and HCCSb compared to HCCP, let alone HCCN. EPR and microwave spectroscopy might provide more insight into the respective ground-state electronic arrangements. The first two electronic transition of these ethynyl pnictinidenes were assigned.

## Experimental Section

### Experimental details

Experiments were performed using standard matrix isolation technique. Prior to the deposition of low temperature matrices, a precursor compound, $HCCAsH_2$ or $HCCSbH_2$ (IR spectra and assignments in SI, S6), was mixed with Ar (Multax 5.0) at the ratio of 1:1000 in a metal vacuum manifold equipped with capacitance manometers. The mixture was then passed through a microleak valve prior to entering a vacuum chamber housing the cold finger of a closed cycle helium cryostat (Advanced Research Systems DE-202SE refrigerator, ultimate temp. of 6 K) where the mixture solidified onto an IR-transparent (CsI) cold target mounted at the end of the cold finger. IR absorption spectra were collected with Bruker Vertex 70 spectrometer featuring a KBr beam splitter and a liq. $N_2$-cooled HgCdTe detector at a resolution of 0.16 $cm^{-1}$. A low-power (Philips UV-C, 11 Watt) mercury lamp was used for UV irradiation. The same experimental procedure was used for electronic spectroscopy with the only changes being replacement of the CsI cold target with sapphire, use of quartz windows on the vacuum shroud housing the cold finger, and monitoring using a UV-3100 spectrophotometer (Shimadzu Scientific Instruments, Japan).

### Computational details

The ground electronic state geometry optimization was performed with two electronic structure methods: CCSD[24] and B3LYP[25]. The bond orders were based on the Natural Bond Orbital analysis[26] of B3LYP electronic density performed with the NBO version 3. The reported anharmonic vibrational frequencies and infrared intensities[27] were obtained with second-order vibrational perturbation theory (VPT2) and employed numerical differentiation of B3LYP electronic energies. The presented energies and shapes of frontier molecular orbitals were obtained with restricted-open computations at the B972[28] level of theory. We used the Dunning-type augmented correlation consistent triple zeta basis set aug-cc-pVTZ[29] for H, C and P atoms. For As, Sb, and Bi atoms we used a similar basis set, aug-cc-pVTZ-PP[30] (with Stuttgart-Koeln small core pseudopotentials[31]), downloaded from the Basis Set Exchange library.[32] The B3LYP, B972, and CCSD computations employed the Gaussian 16 package.[33] The electronic excitation energies presented in Tab. 3 were obtained with two methods : Fock-space CCSD (FS-CCSD)[20] (2,0) sector and generalized active space configuration interaction (GASCI)[21]. For FS-CCSD, the active space was five hole-orbitals for both alpha and beta spins. The FS-CCSD approach includes both static and dynamic correlation and allows for efficient description of states formed by different distributions of electrons over SOMO, HOMO, and HOMO-1 orbitals. For GASCI computations, two active shells were used. The first shell was composed of five orbitals 2 × SOMO, 2 × HOMO, and HOMO-1, while the second shell comprised 29 virtual orbitals. GASCI computations predict the orbital occupation and electronic transition dipole moment together with the excitation energies between the ground and excited states. Relativistic computations for the excited states employed the all-electron triple-zeta relativistic basis sets developed by Dyall[22], with one exception: the FS-CCSD computations for HCCSb employed the Dyall double-zeta basis set. FS-CCSD and GAS computations were performed by DIRAC19[34]. The state-averaged complete active space self-consistent field (CASSCF) non-relativistic computations employed the MULTI code[35] from the Molpro 2012 package.[36] Eight electrons were distributed within the active space consisting of four π orbitals and one σ orbital. All orbitals were optimized during the computations which were performed in the $C_{2v}$ symmetry for both singlet and triplet states. Once again, aug-cc-pVTZ basis sets were applied for H, C, P atoms and aug-cc-pVTZ-PP for As, Sb.

### Synthetic details

We used the reported synthesis of ethynylarsine and ethynylstibine with minor modifications from the previously reported methods.[15] Tributyltin hydride (14.6 g, 50 mmol) was introduced into a two necked round-bottomed flask along with a small amount of duroquinone and fitted on a vacuum line having two U-traps equipped with stopcocks and degassed. The flask was then immersed in a cold bath at 0°C. The first trap was maintained at -60°C to remove high boiling impurities and the second at -110°C to selectively trap ethynylarsine or ethynylstibine. The crude solution of dichloroethynylarsine or -stibine (10 mmol), prepared as previously reported,[16] was slowly introduced with a flex-needle into the reducing mixture over the course of ~10 min. The product was evacuated as soon as it formed and was selectively trapped in the second cold trap. At the end of the addition, the reaction mixture was stirred for 10 min before disconnecting the second trap. The final product was stored in liquid nitrogen until its introduction into the vacuum manifold used for matrix isolation measurements.

## Acknowledgements

We acknowledge the financial support from the PHC Polonium project No. BPN/BFR/2021/1/00028/U/00001. J.C.G. thanks the support from Centre National d'Etudes Spatiales (CNES) and the Programme National Physique et Chimie du Milieu Interstellaire" (PCMI) of CNRS/INSU with INC/INP co-funded by CEA and CNES.

**Keywords:** Stibinidene • arsinidene • pnictinidene • Ethynylstibinidene • photochemistry • HCCAs • matrix isolation • HCCSb • Ethynylarsinidene • Ethynylarsine • Ethynylstibine

[1] E. C. Mitchell, M. E. Wolf, J. M. Turney, H. F. Schaefer III, *Chem. Eur. J.* **2021**, *27*, 14461-14471.

[2] a) C. Wentrup, *Angew. Chem. Int. Ed.* **2018,** *57*, 11508-11521; b) C. Wentrup, *Chem. Rev.* **2017,** *117*, 4562-4623; c) G. Dequirez, V. Pons, P. Dauban, *Angew. Chem. Int. Ed.* **2012,** *51*, 7384-7395; d) M. Soleilhavoup, G. Bertrand, *Chem* **2020**, *6*, 1275-1282; e) M. S. Platz, in *Reactive Intermediate Chemistry*, **2003**, pp. 501-559.

[3] a) X. Li, S. Weissmann, T,-S. Lin, P. P. Gaspar, A. H. Cowley, A. I. Smirnov, *J. Am. Chem. Soc*., **1994**, *116*, 7899-7900; b) G. Bucher, M. L. G. Borst, A. W. Ehlers, K. Lammertsma, S. Ceola, M. Huber, D. Grote and W. Sander, Angew. Chem., Int. Ed. **2005**, 44, 3289–3293; c) A. Mardyukov, D. Niedek and P. R. Schreiner, *J. Am. Chem. Soc.* **2017**, 139, 5019–5022; d) X. Chu, Y. Yang, B. Lu, Z. Wu, W. Qian, C. Song, X. Xu, M. Abe, X. Zeng, *J. Am. Chem. Soc.* **2018,** *140* (42), 13604-13608; e) E. Y. Misochko, A. V. Akimov, D. V. Korchagin, Y. S. Ganushevich, E. A. Melnikov, V. A. Miluykov, *Phys. Chem. Chem. Phys.* **2020**, *22*, 27626-27631.

[4] a) R. N. Dixon, *Can. J. Phys.* **1959**, *37*, 1171.; b) P. Bollmark, I. Kopp, B. Rydh, *J. Mol. Spectrosc.* **1970**, *34*, 487-499.

[5] a) B. Lu, X. Shao, X. Jiang, L. Wang, J. Xue, G. Rauhut, G. Tan, W. Fang, X. Zeng, *J. Am. Chem. Soc.* **2022**, *144*, 21853-21857.; b) D. A. Ramsay, *Nature* **1956**, *178*, 374-375; c) M. Horani, J. Rostas, H. Lefebvre-Brion, *Can. J. Phys.* **1967**, *45*, 3319; d) F. Legay, *Can. J. Phys.* **1960**, *38*, 797.

[6] a) N. Dixon, G. Duxbury, H. M. Lamberton, *Chem. Commun.* **1966**, 460b-461; b) N. Basco, K. K. Yee, *Spectrosc. Lett.* **1968**, *1*, 17-18; c) K. Kawaguchi, E. Hirota, *J. Mol. Spectrosc.* **1984**, *106*, 423-429.

[7] a) S. Yu, D. Fu, A. Shayesteh, I. E. Gordon, D. R. T. Appadoo, P. Bernath, *J. Mol. Spectrosc.* **2005**, *229*, 257-26; b) N. Basco, K. K. Yee, *Spectrosc. Lett.* **1968**, *1*, 13-15; c) P. Bollmark, B. Lindgren, *Chem. Phys. Lett.* **1967**, *1*, 480; d) X. Wang, P. F. Souter, L. Andrews, *J. Phys. Chem. A* **2003**, *107*, 4244-4249.

[8] a) E. Hulthén, H. Neuhaus, Phys. Rev. **1956**, *102*, 1415-1416; b) H. Neuhaus, Z. Naturforsch. **1966**, *21A*, 2113-2114; c) K.-D. Setzer, E. H. Fink, C. Hill, J. M. Brown, *J. Mol. Spectrosc.* **2015**, *312*, 97-109.

[9] D. P. Mukhopadhyay, D. Schleier, S. Wirsing, J. Ramler, D. Kaiser, E. Reusch, P. Hemberger, T. Preitschopf, I. Krummenacher, B. Engels, I. Fischer, C. Lichtenberg, *Chem. Sci.* **2020**, *11*, 7562-7568.

[10] E. Karaev, M. Gerlach, L. Faschingbauer, J. Ramler, I. Krummenacher, C. Lichtenberg, P. Hemberger and I. Fischer, *Chem. Eur. J.* 2023, e202300837.

[11] a) F. Dielmann, O. Back, M. Henry-Ellinger, P. Jerabek, G. Frenking and G. Bertrand, *Science*, **2012**, 337, 1526-1528; (b) J. Sun, J. Abbenseth, H. Verplancke, M. Diefenbach, B. de Bruin, D. Hunger, C. Würtele, J. van Slageren, M. C. Holthausen and S. Schneider, *Nat. Chem.*, **2020**, 12, 1054-1059.

[12] a) R. Waterman, *Chem* **2016**, *1*, 27-29; b) L. Liu, D. A. Ruiz, D. Munz, G. Bertrand, *Chem.* **2016,** *1*, 147-153.

[13] a) A. H. Cowley, N. C. Norman, M. Pakulski, D. Bricker, D. R. Russell, *J. Am. Chem. Soc.* **1985**, *107*, 8211-8218; b) L. Dostál, *Coord. Chem. Rev.* **2017**, *353*, 142-158; c) R. C. Smith, P. Gantzel, A. L. Rheingold, J. D. Protasiewicz, *Organometallics* **2004**, *23*, 5124-5126..

[14] a) A. J. Arduengo III, J. C. Calabrese, A. H. Cowley, H. V. R. Dias, J. R. Goerlich, W. J. Marshall, B. Riegel, *Inorganic Chemistry* **1997**, *36*, 2151-2158; b) P. Šimon, F. de Proft, R. Jambor, A. Růžička, L. Dostál, *Angew. Chem. Int. Ed.* **2010**, *49*, 5468-5471; c) I. Vránová, V. Kremláček, M. Erben, J. Turek, R. Jambor, A. Růžička, M. Alonso, L. Dostál, *J. Chem. Soc., Dalton trans.* **2017**, *46*, 3556-3568; d) I. Vránová, M. Alonso, R. Jambor, A. Růžička, M. Erben, L. Dostál, *Chem. Eur. J.* **2016**, *22*, 7376-7380; e) A. Doddi, M. Weinhart, A. Hinz, D. Bockfeld, J. M. Goicoechea, M. Scheer, M. Tamm, *Chem. Commun.* **2017**, *53*, 6069-6072; f) J. Hyvl, W. Y. Yoshida, A. L. Rheingold, R. P. Hughes, M. F. Cain, *Chem. Eur. J.* **2016**, *22*, 17562-17565; g) D. Raiser, K. Eichele, H. Schubert, L. Wesemann, *Chem. Eur. J.* **2021**, *27*, 14073-14080; h) G. Wang, L. A. Freeman, D. A. Dickie, R. Mokrai, Z. Benkő, R. J. Gilliard Jr., *Chem. Eur. J.* **2019**, *25*, 4335-4339; i) M. S. M. Philipp, U. Radius, *Z. Anorg. Allg. Chem.* **2022**, *648*, e202200085; j) S. Takahiro, A. Yoshimitsu, T. Nobuhiro, O. Renji, T. Norihiro, *Chem. Lett.* **2001**, *30*, 42-43; k) C. L. Dorsey, R. M. Mushinski, T. W. Hudnall, *Chem. Eur. J.* **2014**, *20*, 8914-8917.

[15] A.-L. Lawzer, T. Custer, J.-C. Guillemin, R. Kołos, *Angew. Chem. Int. Ed.* **2021**, *60*, 6400-6402.

[16] a) J.-C. Guillemin, L. Lassalle, P. Drean, G. Wlodarczak, J. Demaison, *J. Am. Chem. Soc.* **1994**, *116*, 8930-8936; b) S. Legoupy, L. Lassalle, J. C. Guillemin, V. Metail, A. Senio, G. Pfister-Guillouzo, *Inorg. Chem.* **1995**, *34*, 1466-1471.

[17] a) V. M. Rayón, C. Barrientos, P. Redondo, A. Largo, *Chem. Phys. Lett.* **2010**, *485*, 286-289; b) M. Z. Milovanović, S. V. Jerosimić, *Chem. Phys. Lett.* **2013**, *565*, 28-34.

[18] a) G. Maier, H. P. Reisenauer, K. Rademacher, *Chem. Eur. J.* **1998**, *4*, 1957-1963; b) X. Zeng, H. Beckers, J. Seifert, K. Banert, *Eur. J. Org. Chem.* **2014**, *2014*, 4077-4082; c) A. Dendramis, G. E. Leroi, *J. Chem. Phys.* **1977**, *66*, 4334-4340; d) M. Nakajima, H. Toyoshima, S. Sato, K. Tanaka, K. Hoshina, H. Kohguchi, Y. Sumiyoshi, Y. Ohshima, Y. Endo, *J. Chem. Phys.* **2013**, *138*, 164309.

[19] a) F. X. Brown, S. Saito, S. Yamamoto, *J. Mol. Struct.* **1990**, 143, 203-208; b) I. K. Ahmad, H. Ozeki, S. Saito, *J. Chem. Phys.* **1997**, *107*, 1301-1307.

[20] L. Visscher, E. Eliav. U. Kaldor, *J. Chem. Phys.* **2001**, *115*, 9720-9726.

[21] a) T. Fleig, J. Olsen, L. Visscher, *J. Chem. Phys.* **2003**, *119*, 2963-2971; b) T. Fleig, H. J. A. Jensen, J. Olsen, L. Visscher, *J. Chem. Phys.* **2006**, *124*, 104106; c) J. Olsen, P. Jørgensen, J. Simons, *Chem. Phys. Lett.* **1990**, *169*, 463-4721; d) S. Knecht, H. J. A. Jensen, T. Fleig, *J. Chem. Phys.* **2010**, *132*, 014108.

[22] K. G. Dyall, *Theor. Chem. Acc.* **2006**, *115*, 441-447.

[23] a) R. A. Bernheim, R. J. Kempf, P. W. Humer, P. S. Skell, *J. Chem. Phys.* **1964**, *41*, 1156-1157; b) R. A. Bernheim, R. J. Kempf, J. V. Gramas, P. S. Skell, *J. Chem. Phys.* **1965**, *43*, 196-200.

[24] a) J. Cížek in *Advances in Chemical Physics*, *Vol. 14* (Eds.: P. C. Hariharan), Wiley Interscience, New York, **1969**, pp. 35; b) G. D. Purvis III, R. J. Bartlett, *J. Chem. Phys.* **1983**, *76*, 1910-1918; c) G. E. Scuseria, C. L. Janssen, H. F. Schaefer III, *J. Chem. Phys.* **1988**, *89*, 7382-7387; d) G. E. Scuseria, C. L. Janssen, H. F. Schaefer III, *J. Chem. Phys.* **1989**, *90*, 3700-3703; e) J. Thyssen. Development and Applications of Methods for Correlated Relativistic Calculations of Molecular Properties. PhD thesis, University of Southern Denmark, **2001.**

[25] A. D. Becke, *J. Chem. Phys*. **1993**, *7*, 5648-5652.

[26] a) A. E. Reed, F. Weinhold, *J. Chem. Phys.* **1985**, *83*, 1736-1740; b) A. E. Reed, R. B. Weinstock, F. Weinhold, *J. Chem. Phys.* **1985**, *83*, 735-746; c) J. P. Foster, F. Weinhold, *J. Am. Chem. Soc.* **1980**, *102*, 7211-7218; d) F. Weinhold, J. E. Carpenter in The Structure of Small Molecules and Ions (Eds R. Naaman, Z. Vager), Plenum, **1988**, pp.227.

[27] a) J. Bloino, V. Barone, *J. Chem. Phys.* **2012**, *136*, 124308; b) J. Bloino, *J. Phys. Chem. A* **2015**, *119*, 5269-5287 c) V. Barone, *J. Chem. Phys.* **2005**, *122*, 014108.

[28] P. J. Wilson, T. J. Bradley, and D. J. Tozer, J. Chem. Phys., **2001**, *115*. 9233-9242

[29] a) T. H. Dunning Jr., *J. Chem. Phys.* **1989**, *90*, 1007-1023; b) R. A. Kendall, T. H. Dunning Jr., R. J. Harrison, *J. Chem. Phys.* **1992**, *96*, 6796-6806.

[30] a) D. E. Woon, T. H. Dunning Jr., *J. Chem. Phys.* **1993**, *98*, 1358-1371; b) K. A. Peterson, *J. Chem. Phys.* **2003**, *119*, 11099-11112.

[31] B. Metz, H. Stoll, M. Dolg, *J. Chem. Phys.* **2000**, *113*, 2563-2569

[32] B. P. Pritchard, D. Altarawy, B. Didier, T. D. Gibson, T. L. Windus, *J. Chem. Inf. Model.* **2019**, *59*, 4814-4820.

[33] Gaussian 16, Revision B.01, M. J. Frisch, G. W. Trucks, H. B. Schlegel, G. E. Scuseria, M. A. Robb, J. R. Cheeseman, G. Scalmani, V. Barone, G. A. Petersson, H. Nakatsuji, X. Li, M. Caricato, A. V. Marenich, J. Bloino, B. G. Janesko, R. Gomperts, B. Mennucci, H. P. Hratchian, J. V. Ortiz, A. F. Izmaylov, J. L. Sonnenberg, D. Williams-Young, F. Ding, F. Lipparini, F. Egidi, J. Goings, B. Peng, A. Petrone, T. Henderson, D. Ranasinghe, V. G. Zakrzewski, J. Gao, N. Rega, G. Zheng, W. Liang, M. Hada, M. Ehara, K. Toyota, R. Fukuda, J. Hasegawa, M. Ishida, T. Nakajima, Y. Honda, O. Kitao, H. Nakai, T. Vreven, K. Throssell, J. A.

Montgomery, Jr., J. E. Peralta, F. Ogliaro, M. J. Bearpark, J. J. Heyd, E. N. Brothers, K. N. Kudin, V. N. Staroverov, T. A. Keith, R. Kobayashi, J. Normand, K. Raghavachari, A. P. Rendell, J. C. Burant, S. S. Iyengar, J. Tomasi, M. Cossi, J. M. Millam, M. Klene, C. Adamo, R. Cammi, J. W. Ochterski, R. L. Martin, K. Morokuma, O. Farkas, J. B. Foresman, and D. J. Fox, Gaussian, Inc., Wallingford CT, **2016**.

[34] DIRAC, a relativistic ab initio electronic structure program, Release DIRAC19, 2019, written by A. S. P. Gomes, T. Saue, L. Visscher, H. J. Aa. Jensen, and R. Bast, with contributions from I. A. Aucar, V. Bakken, K. G. Dyall, S. Dubillard, U. Ekström, E. Eliav, T. Enevoldsen, E. Faßhauer, T. Fleig, O. Fossgaard, L. Halbert, E. D. Hedegård, B. Heimlich–Paris, T. Helgaker, J. Henriksson, M. Iliaš, Ch. R. Jacob, S. Knecht, S. Komorovský, O. Kullie, J. K. Lærdahl, C. V. Larsen, Y. S. Lee, H. S. Nataraj, M. K. Nayak, P. Norman, G. Olejniczak, J. Olsen, J. M. H. Olsen, Y. C. Park, J. K. Pedersen, M. Pernpointner, R. di Remigio, K. Ruud, P. Sałek, B. Schimmelpfennig, B. Senjean, A. Shee, J. Sikkema, A. J. Thorvaldsen, J. Thyssen, J. van Stralen, M. L. Vidal, S. Villaume, O. Visser, T. Winther, and S. Yamamoto, available at http://dx.doi.org/10.5281/zenodo.3572669, see also http://www.diracprogram.org.

[35] a) P. J. Knowles, N. C. Handy, *Chem. Phys. Chem.* **1984**, *111*, 315-321; b) H.-J. Werner, W. Meyer, *J. Chem. Phys.* **1980**, *73*, 2342-2356; c) H.-J. Werner, W. Meyer, *J. Chem. Phys.* **1981**, *74*, 5793-5801.

[36] a) H.-J. Werner, P. J. Knowles, G. Knizia, F. R. Manby and M. Schütz, *Wiley Interdiscip. Rev. Comput. Mol. Sci.* **2012**, *2*, 242-253; b) MOLPRO, version , a package of ab initio programs, H.-J. Werner, P. J. Knowles, P. Celani, W. Györffy, A. Hesselmann, D. Kats, G. Knizia, A. Köhn, T. Korona, D. Kreplin, R. Lindh, Q. Ma, F. R. Manby, A. Mitrushenkov, G. Rauhut, M. Schütz, K. R. Shamasundar, T. B. Adler, R. D. Amos, S. J. Bennie, A. Bernhardsson, A. Berning, J. A. Black, P. J. Bygrave, R. Cimiraglia, D. L. Cooper, D. Coughtrie, M. J. O. Deegan, A. J. Dobbyn, K. Doll and M. Dornbach, F. Eckert, S. Erfort, E. Goll, C. Hampel, G. Hetzer, J. G. Hill, M. Hodges and T. Hrenar, G. Jansen, C. Köppl, C. Kollmar, S. J. R. Lee, Y. Liu, A. W. Lloyd, R. A. Mata, A. J. May, B. Mussard, S. J. McNicholas, W. Meyer, T. F. Miller III, M. E. Mura, A. Nicklass, D. P. O'Neill, P. Palmieri, D. Peng, K. A. Peterson, K. Pflüger, R. Pitzer, I. Polyak, M. Reiher, J. O. Richardson, J. B. Robinson, B. Schröder, M. Schwilk and T. Shiozaki, M. Sibaev, H. Stoll, A. J. Stone, R. Tarroni, T. Thorsteinsson, J. Toulouse, M. Wang, M. Welborn and B. Ziegler, see https://www.molpro.net.

10.1002/chem.202300887

WILEY-VCH

RESEARCH ARTICLE

## Entry for the Table of Contents

## Entry for the Table of Contents

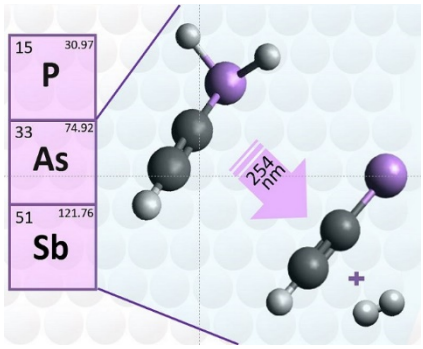


Triplet ethynylarsinidene (HCCAs) and ethynylstibinidene (HCCSb) were generated photochemically in argon matrices from their corresponding pnictines. Electronic structures of these species are compared with HCCN and HCCP in light of their vibrational and electronic spectra and with support from theory.

Institute and/or researcher Twitter usernames: @ICHF_PAN, @Gronowski_M, @GElavenil